Received: 24 November 2020 | Revised: 8 March 2021 | Accepted: 11 March 2021

DOI: 10.1111/cas.14883

ORIGINAL ARTICLE

Cancer Science WILEY

# miRNAs derived from circulating small extracellular vesicles as diagnostic biomarkers for nasopharyngeal carcinoma

Li Jiang[1] | Yong Zhang[1] | Bo Li[1] | Min Kang[1] | Zhendong Yang[1] | Chunyu Lin[2] | Kai Hu[1] | Zhuxin Wei[1] | Meng Xu[1] | Jinglin Mi[1] | Rensheng Wang[1] | Fang Wu[1]

[1]Department of Radiation Oncology, The First Affiliated Hospital of Guangxi Medical University, Nanning, China

[2]Department of Clinical Laboratory, The First Affiliated Hospital of Guangxi Medical University, Nanning, China

**Correspondence**
Fang Wu, Rensheng Wang, Department of Radiation Oncology, The First Affiliated Hospital of Guangxi Medical University, 6 Shuangyong Road, Nanning 530021, Guangxi, China.
Emails: wufang2022@163.com; 13807806008@163.com

**Funding information**
the Key Research and Development Program of Guangxi, Grant/Award Number: Guike AB18281003; Guangxi Medical and Health Appropriate Technology Development and Promotion Application Project, Grant/Award Number: S2017020; Middle-aged and Young Teachers' Basic Ability Promotion Project of Guangxi, Grant/Award Number: 2018KY0134; Guangxi Science and Technology Program Project, Grant/Award Number: GK AD17129013; National Natural Science Foundation of China, Grant/Award Number: 82060019 and 82060494

## Abstract

The microRNAs (miRNAs) in circulating small extracellular vesicles (sEVs) have been suggested as potential biomarkers in cancer diagnosis. This study was designed to evaluate the circulating sEV-derived miRNAs as biomarkers for the diagnosis of nasopharyngeal carcinoma (NPC). We compared the miRNA profiles in plasma-derived sEVs between 16 patients with NPC and 5 healthy controls (HCs). A distinct set of miRNAs that were differentially expressed between patients with NPC and HCs was determined by means of integrative bioinformatics approaches. Kyoto Encyclopedia of Genes and Genomes (KEGG) enrichment pathway analysis revealed that the target genes of the differentially expressed miRNAs (DEMs) were mainly involved in cancer-associated signaling pathways. Seven representative DEMs were selected and further validated in an additional 60 patients with NPC and 40 HCs using quantitative reverse-transcription PCR analysis (qRT-PCR). Receiver operating characteristic (ROC) curve analysis was used to assess the accuracy of the sEV-miRNA-based model for diagnosis. The 3 miRNA-based model, comprising miR-134-5p, miR-205-5p, and miR-409-3p, showed good discriminating power with an area under the curve (AUC) value of 0.88 in the training set and 0.91 in the validation set. Furthermore, the diagnostic model had an excellent classification ability to distinguish patients with NPC at different clinical stages or Epstein-Barr virus infection status from HCs. In conclusion, our findings indicated that sEV-derived miRNA levels were altered in the plasma of patients with NPC in comparison with those in HCs. The model based on the 3 sEV-derived miRNAs could potentially act as an alternative or complementary approach for diagnosing NPC.

KEYWORDS

biomarker, diagnosis, microRNA, nasopharyngeal carcinoma, small extracellular vesicle

**Abbreviations:** ATM, ataxia telangiectasia-mutated; AUC, area under the curve; DEM, differentially expressed miRNA; EBV, Epstein-Barr virus; EMT, epithelial-mesenchymal transition; GO, Gene Ontology; HCs, healthy controls; JAK1, Janus kinase 1; KEGG, Kyoto Encyclopedia of Genes and Genomes; NPC, nasopharyngeal carcinoma; ROC, receiver operating characteristic; SEC, size exclusion chromatography; sEVs, small extracellular vesicles; STAT3, signal transducer and activator of transcription 3; TPM, transcripts per kilobase of exon model per million mapped reads.

Li Jiang and Yong Zhang contributed equally to this work as co-first authors.

This study was designed to evaluate circulating sEV-derived miRNAs as biomarkers for the diagnosis of nasopharyngeal carcinoma (NPC). Our findings indicated that sEV-derived miRNA levels were altered in the plasma of patients with NPC compared with those in HCs. The model based on the 3 sEV-derived miRNAs could potentially act as an alternative or complementary approach for diagnosing NPC.

## 1 | INTRODUCTION

Nasopharyngeal carcinoma (NPC), a malignant epithelial tumor originating from the nasopharynx epithelium, has a high reported prevalence in the south of China.[1] In particular, NPC tends to be aggressive in nature and therefore is usually diagnosed as locoregional advanced disease.[2] Radiotherapy has become the mainstream treatment modality for nonmetastatic NPC, due to its inherent radiosensitivity and anatomic constraints. The advancement in detection methods and treatment strategies has led to a decrease in the mortality of NPC over the past decades. Many patients with NPC, however, are diagnosed at an advanced stage of the disease, which has been associated with treatment failure, therefore there is a need to detect a novel biomarker to ensure the early diagnosis of NPC to predict treatment outcomes.[3]

Small extracellular vesicles (sEVs) are lipid bilayer vesicles of 40-100 nm in diameter that contain miRNAs and are known to play an important role in cell communication.[4] More specifically, sEVs that are secreted from donor cells and affect target cells[5,6] are stable in body fluids and transfer functional miRNAs and proteins as a means of exchanging biological information.[7] miRNAs, which are a major substances in sEVs, play a critical role in regulating gene expression, tumor growth, and resistance to cancer therapy[8,9] and are well protected from degradation by the sEV membrane. Moreover, they are also known to be expressed in sEVs under pathological conditions.[10] Therefore, sEVs and their miRNAs could be promising novel cancer biomarkers. There is growing evidence indicating the involvement of sEVs in NPC.[11] For instance, some miRNAs could be identified in serum but not in exosomes, indicating a discrepancy between the expression of miRNAs in the serum or in plasma and exosomes.[12] To date, there have been few studies on the systematic screening of plasma sEV-derived miRNAs related to NPC diagnosis. In this study, we identified sEV-derived miRNAs as biomarkers for the diagnosis of NPC.

## 2 | MATERIALS AND METHODS

### 2.1 | Patients and collection of clinical samples

In total, 16 patients with NPC, who received radiotherapy and chemotherapy at the Department of Radiation Oncology, The First Affiliated Hospital of Guangxi Medical University between July and November 2019, were enrolled in this study along with 5 HCs. All participants were subjected to miRNA sequencing. Additionally, 60 patients with NPC and 40 HCs were enrolled for qPCR validation. Inclusion criteria were as follows: 1) patients initially diagnosed with nonmetastatic NPC (stages I to IVa); 2) patients treated with intensity-modulated radiotherapy and platinum-based chemotherapy at the First Affiliated Hospital of Guangxi Medical University; and 3) availability of peripheral blood samples. Exclusion criteria were: 1) diagnosis with distant metastasis during treatment; and 2) history of any other malignant disease. Additionally, the inclusion criteria for HCs were: 1) no history of malignant disease; 2) a Karnofsky performance status ≥ 90; and 3) a willingness to undergo peripheral blood sampling. All medical records were reviewed retrospectively, and the TNM classification was restaged according to the 8th edition of the International Union against Cancer/American Joint Committee on Cancer (UICC/AJCC) classification system. Informed consent was obtained from all participants, and the research protocol was approved by the Ethical Review Committee of the First Affiliated Hospital of Guangxi Medical University.

### 2.2 | Isolation of plasma sEVs

Blood samples were collected from all subjects in K2-EDTA tubes (BD Vacutainer, New Jersey, NJ, USA) and processed within 2 h after collection. Plasma samples were collected through consecutive centrifugation steps at 500 × *g* for 10 min, 2000 × *g* for 10 min, followed by 3000 × *g* for 30 min at 4°C to minimize contamination by platelets. Plasma samples were stored at −80°C until further analysis, avoiding more than 2 freeze-thaw cycles.

Small extracellular vesicles were isolated from plasma using SEC, as previously described, with minor modifications.[13] Briefly, 2 mL plasma samples were passed through a 0.22-μm filter (Corning, Germany) to remove cell debris and large extracellular vesicles. The supernatant was loaded into a Sepharose based CL-2B column (Echo9103A-10 ml; Echo Biotech, Beijing, China), and eluted using sterile PBS after all samples were into the column and no fluid flowed out from the column bottom. Eluted fractions 4–7 (0.5 mL each) were collected in a total volume of 2 mL. The effluents were concentrated to 200 μL using 100 kDa ultrafiltration tubes centrifuged at 4000 × *g* for 15 min.

### 2.3 | Identification of plasma sEVs

A total of 10 μL sEV-enriched fraction was dropped on a copper mesh and incubated at 25°C for 10 min. The sEV-enriched fraction

was negative stained using uranyl acetate for 1 min. Subsequently, the sample was air dried for 2 min under incandescent light. Microphotographs were acquired using a transmission electron microscope (H-7650, Hitachi Ltd., Tokyo, Japan).

Nanoparticle tracking analysis (NTA) was performed on the sEV-enriched fractions using ZetaView PMX 110 (Particle Metrix, Meerbusch, Germany) equipped with a 405 nm laser module. The obtained data were analyzed using the corresponding software (ZetaView 8.02.28). To measure the size, concentration, and number of particles in the light-scattering instrument, samples were diluted by PBS at concentrations between $1 \times 10^7$/mL and $1 \times 10^9$/mL.

Western blot analysis was performed to identify sEV-positive (TSG101, sc-13611, Santa Cruz, CA, USA; CD63, sc-5275, Santa Cruz; and Alix, sc-53540, Santa Cruz) and negative (calnexin, 10427-2-AP, Promega, Madison, WI, USA) markers. In brief, the sEV supernatant was denatured in 5× sodium dodecyl sulfonate (SDS) buffer and subjected to western blot analysis (10% SDS-polyacrylamide gel electrophoresis; 50 μg protein/lane) using the above rabbit polyclonal antibodies. Proteins were then visualized on a Tanon 4600 automatic chemiluminescence image analysis system (Tanon, Shanghai, China).

## 2.4 | Total RNA extraction and RNA sequencing

Total RNA was extracted and purified from plasma sEVs using the miRNeasy® Mini kit (Qiagen, cat. no. 217 004) according to the standard protocol. RNA concentration and purity were assessed using the RNA Nano 6000 Assay Kit of the Agilent Bioanalyzer 2100 System (Agilent Technologies, CA, USA). An miRNA sequencing library was prepared from the total RNA in each sample according to the following steps. A total of 1–500 ng RNA per sample was used as input material for small RNA sample preparations. Sequencing libraries were generated using a QIAseq miRNA Library Kit (Qiagen, Frederick, MD, USA) following the manufacturer's instructions, with index codes being added to attribute sequences to each sample. Finally, library quality was assessed using the Agilent Bioanalyzer 2100 and qPCR. Clustering of the index-coded samples was performed on an acBot Cluster Generation System using the TruSeq PE Cluster Kitv3-cBot-HS (Illumina, San Diego, CA, USA) following the manufacturer's instructions. After cluster generation, paired-end reads were generated, and the library preparations were sequenced on an Illumina HiSeq platform.

## 2.5 | Bioinformatic analysis of miRNA sequencing data

Using the tools of the Bowtie software, the clean reads were aligned with sequences from the Silva, GtRNAdb, Rfam, and Repbase databases, using filters for ribosomal RNA, transfer RNA, small nuclear RNA, small nucleolar RNA, and other noncoding RNA, and repeats. The remaining reads were used to detect known miRNAs, compared with the miRbase, and new miRNAs, compared with the Human Genome (GRCh38). Read counts for each miRNA were obtained from the mapping results, and the transcripts per kilobase of exon model per million mapped reads (TPM) were calculated. GO enrichment analysis of target genes of differentially expressed miRNAs was implemented using topGO R packages. We used the KOBAS software (version x.0) to statistically evaluate the enrichment of differentially expressed genes in KEGG pathways.[14,15]

## 2.6 | miRNA qRT-PCR

The PrimeScript™ RT reagent kit (Perfect Real Time) (TaKaRa, RR037A) was used to synthesize cDNA. The abundance of target gene expression was detected using a TaqMan® probe using real-time qPCR (TAKARA, RR390A). As a template, 2 μL cDNA was used for each PCR reaction. The sequences of primers and probes are shown in Table S1.

## 2.7 | Statistical analysis

Logistic regression analysis was applied to build models consisting of a group of candidate diagnostic miRNAs. The ROC curve analysis

**TABLE 1** Clinical characteristics of patients with NPC and healthy controls

| | RNA sequencing set (N = 21) | PCR validation set (N = 100) |
|---|---|---|
| **Gender** | | |
| Male | 16 | 68 |
| Female | 5 | 32 |
| **Age (years)** | 45.29 ± 11.71 | 43.52 ± 12.72 |
| **T stage** | | |
| T1 | 4 | 12 |
| T2 | 4 | 18 |
| T3 | 3 | 9 |
| T4 | 5 | 21 |
| **N stage** | | |
| N0 | 3 | 12 |
| N1 | 5 | 24 |
| N2 | 4 | 15 |
| N3 | 4 | 9 |
| **Clinical stage** | | |
| I | 2 | 5 |
| II | 6 | 18 |
| III | 2 | 12 |
| IVa | 6 | 25 |
| EBV DNA detection (>400 copies/ml) | 8 | 35 |

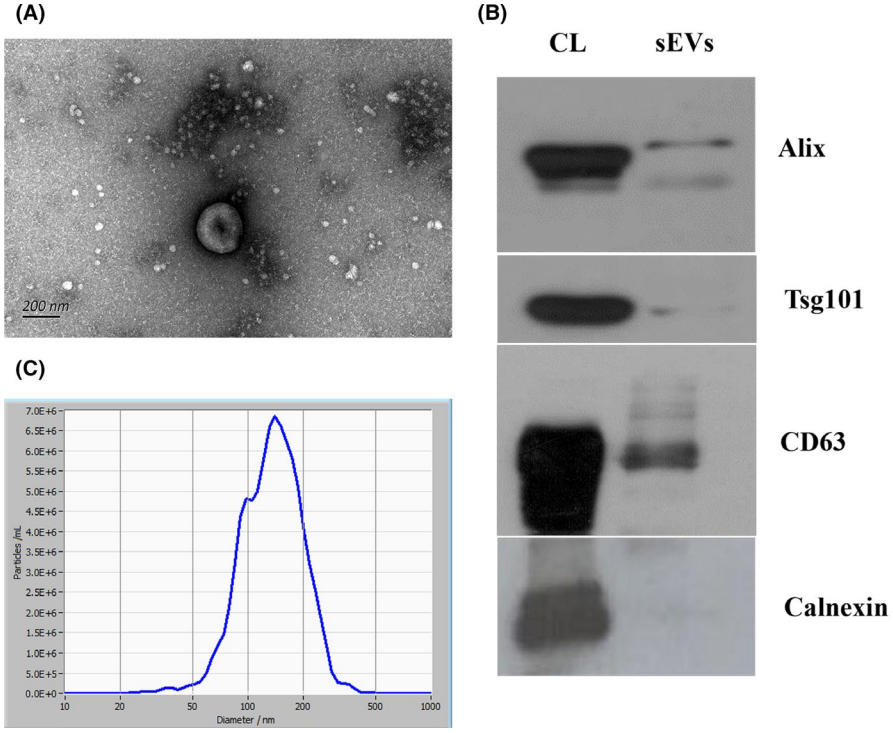


**FIGURE 1** Characteristics of plasma-derived sEVs. A, Images of transmission electron microscopy showing that sEVs are bowl shaped. Scale, 200 nm. B, Western blot analysis showing the expression of CD63, TSG101, and Alix, and the absence of calnexin. C, Nanoparticle tracking analysis showing the size distribution of sEVs; mean size was 144.6 nm. CL, cell lysates

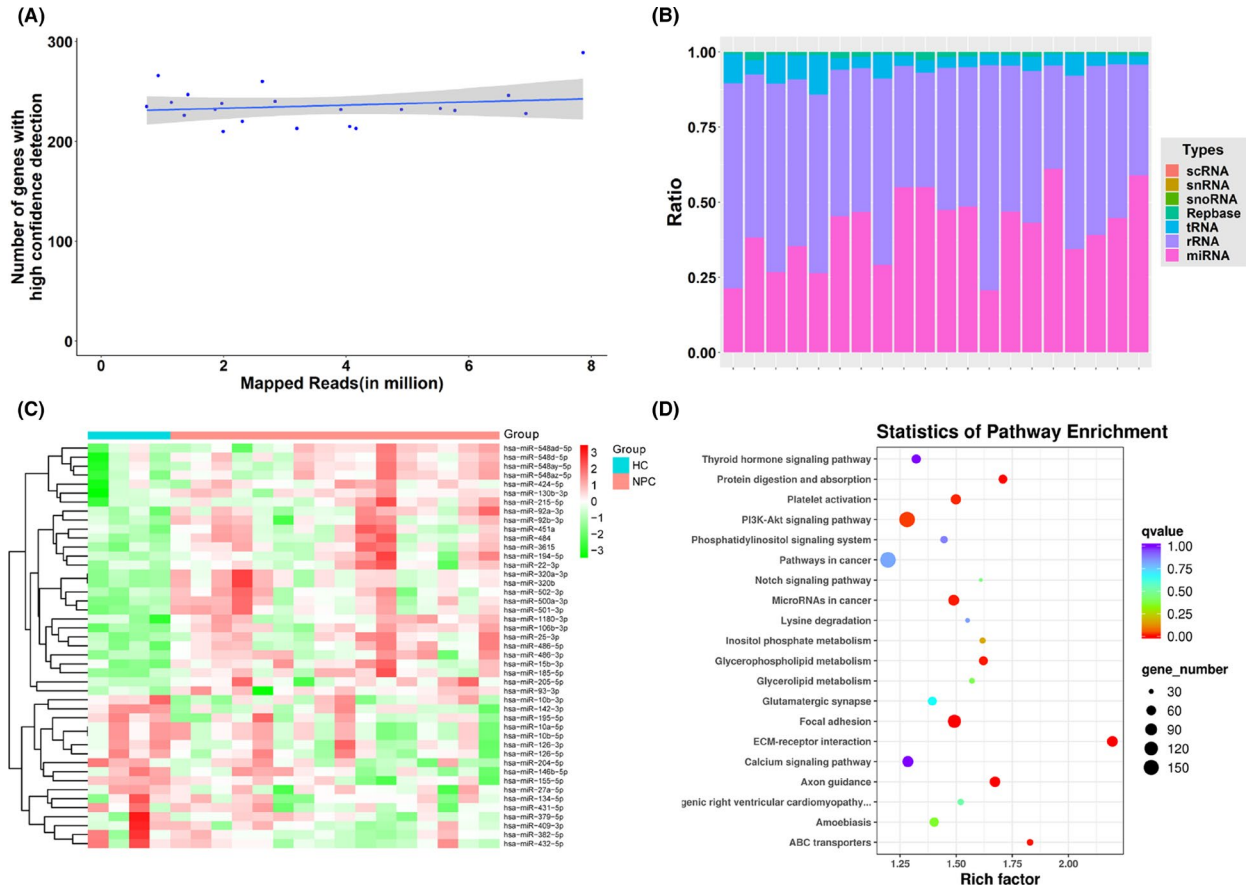


**FIGURE 2** Characterization of plasma-derived sEV-miRNAs in patients with NPC. A, Sequencing saturation analysis. The number of effective miRNAs (TPM > 10) detected in the sequencing data in each sample. B, Distribution of mappable small RNAs by NGS. C, Heatmap of differentially expressed miRNAs in plasma sEVs. D, Bubble diagram for analysis of genes targeted by the differentially expressed miRNAs in KEGG analysis. scRNA, small cytoplasmic RNA; snRNA, small nuclear RNA; snoRNA, small nucleolar RNA; Repbase, repeat sequence; tRNA, transfer RNA; rRNA, ribosomal RNA; miRNA, microRNA; NPC, nasopharyngeal carcinoma; HC, healthy control

was carried out to assess the performance of the model by calculating their AUC. Statistical tests were performed using R v.3.5.1 (www.r-project.org). An UpSet plot was also constructed using the 'UpSetR' R package to overlap miRNAs in 5 comparisons. All tests were 2-tailed and the false discovery rate was controlled for multiple comparisons. $P < .05$ was considered statistically significant. The plyr and reshape2 packages were used for data sorting and restructuring. The UpSetR, pheatmap, and ggplot2 packages were used for visualization of results.

## 3 | RESULTS

### 3.1 | Identification and characterization of plasma-derived sEVs

We isolated sEVs from the plasma of patients with NPC and HCs using SEC and characterized them by transmission electron microscopy (TEM), NTA, and western blotting. The clinicopathological information of the participants is summarized in Table 1. Morphological analysis of the plasma-derived sEVs using TEM showed the typical bowl-shaped morphology of sEVs (Figure 1A). The isolated sEVs were highly enriched in CD63, TSG101, and Alix sEV-specific markers, whereas calnexin, a negative sEV marker, was not detected (Figure 1B). In addition, analysis using NTA showed that the mean size of sEVs was 144.6 nm (Figure 1C).

### 3.2 | Comparison of miRNA profiling and bioinformatic analysis of sEV-derived miRNAs between patients with NPC and HCs

Next-generation sequencing performed on samples from 16 patients with NPC and 5 HCs revealed the presence of a total of 1197 miRNAs, of which 1159 were known miRNAs. Through quality control, we determined that the average clean data of each sample was 8.73 M. We measured the quality of miRNA sequencing by distribution and saturation, as shown in Figure 2A,B. We included miRNAs with a median TPM > 10 for subsequent analysis to avoid bias induced by miRNAs with relatively low expression levels. Analysis of differentially expressed miRNAs revealed that ($|FC| \geq 1.5$, $P \leq .05$) 28 miRNAs were upregulated, whereas 17 were downregulated in patients with NPC compared with those in HCs (Table S2).

We used hierarchical clustering to distinguish the miRNA expression profiles between patients with NPC and HCs (Figure 2C). Moreover, to show the potential biological functions and signaling pathways of target genes of DEMs (patients with NPC vs. HCs), we performed GO and KEGG pathway analyses using target genes. The cancer-associated pathways related to the regulated target genes are shown in Figure 2D. The most enriched categories and the enrichment scores in biological process, cellular component, and molecular function are shown in Figure S1A-C. The genes targeted by DEMs were mainly enriched in biological functions, such as cell adhesion, cell migration, axon guidance, and ATP binding.

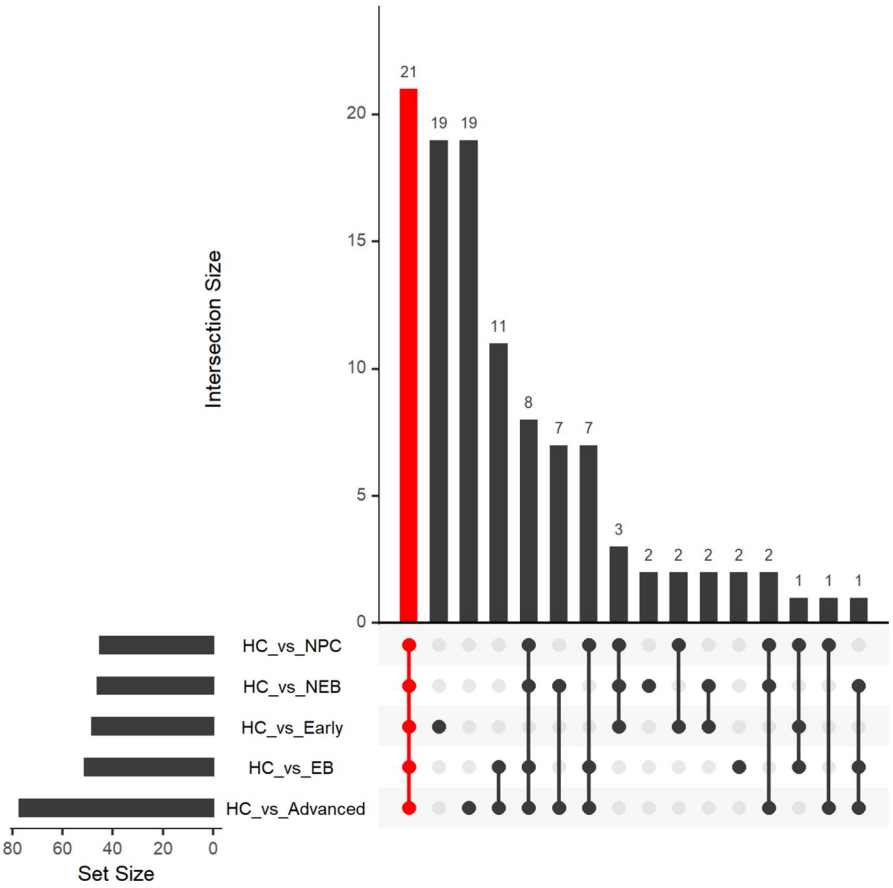


**FIGURE 3** UpSet intersection diagram. Five comparisons are shown in the UpSet plot. The numbers on the bars show the numbers of overlapping miRNAs in the corresponding comparison

**TABLE 2** Assessment scale for the selection of NPC diagnostic biomarker candidates from 21 miRNAs

| ID | Literature | FC ≥2 or FC ≤0.5 | Expression>=50 | *P*-value | FDR | $Log_2$ FC | Regulation |
|---|---|---|---|---|---|---|---|
| hsa-miR-134-5p | 3 | 1 | 0 | 1.652E-03 | 0.208221 | -1.99721 | Down |
| hsa-miR-205-5p | 3 | 1 | 1 | 4.531E-03 | 0.333936 | 3.138441 | Up |
| hsa-miR-409-3p | 2 | 1 | 1 | 4.370E-05 | 0.023441 | -2.12066 | Down |
| hsa-miR-484 | 2 | 1 | 1 | 6.206E-03 | 0.359288 | 1.404613 | Up |
| hsa-miR-486-3p | 2 | 0 | 1 | 2.905E-02 | 0.621316 | 0.864261 | Up |
| hsa-miR-486-5p | 2 | 1 | 1 | 4.456E-03 | 0.333936 | 1.079406 | Up |
| hsa-miR-92b-3p | 2 | 1 | 1 | 1.899E-02 | 0.528252 | 1.117708 | Up |
| hsa-miR-130b-3p | 2 | 1 | 0 | 1.471E-02 | 0.473991 | 1.063487 | Up |
| hsa-miR-195-5p | 2 | 0 | 1 | 8.500E-03 | 0.359288 | -0.79029 | Down |
| hsa-miR-320b | 2 | 0 | 1 | 7.203E-03 | 0.359288 | 0.756499 | Up |
| hsa-miR-379-5p | 2 | 1 | 0 | 7.724E-04 | 0.12457 | -1.85042 | Down |
| hsa-miR-106b-3p | 1 | 0 | 1 | 2.039E-03 | 0.230258 | 0.925956 | Up |
| hsa-miR-204-5p | 1 | 1 | 1 | 2.709E-03 | 0.272916 | -1.13235 | Down |
| hsa-miR-3615 | 1 | 1 | 1 | 1.606E-02 | 0.489985 | 1.000903 | Up |
| hsa-miR-432-5p | 1 | 1 | 1 | 7.010E-05 | 0.023441 | -2.11438 | Down |
| hsa-miR-15b-3p | 0 | 1 | 1 | 9.265E-03 | 0.360713 | 1.202865 | Up |
| hsa-miR-185-5p | 0 | 1 | 1 | 5.165E-03 | 0.333936 | 1.053123 | Up |
| hsa-miR-320a-3p | 0 | 0 | 1 | 8.036E-03 | 0.359288 | 0.746225 | Up |
| hsa-miR-382-5p | 0 | 1 | 1 | 1.038E-04 | 0.023441 | -1.73895 | Down |
| hsa-miR-500a-3p | 0 | 1 | 1 | 5.216E-03 | 0.333936 | 1.036111 | Up |
| hsa-miR-501-3p | 0 | 1 | 0 | 3.143E-03 | 0.272916 | 1.173655 | Up |

*Note:* The literature score indicates the correlation between miRNAs and NPC that has been reported in previous studies. Score 0, no literature related to NPC found; score 1, only mentioned in literature on NPC; score 2, the upregulation or downregulation of miRNA was reported in NPC-associated literatures; score 3, the role of the miRNA in NPC had been investigated.

Abbreviation: FC, fold change; FDR, false discovery rate.

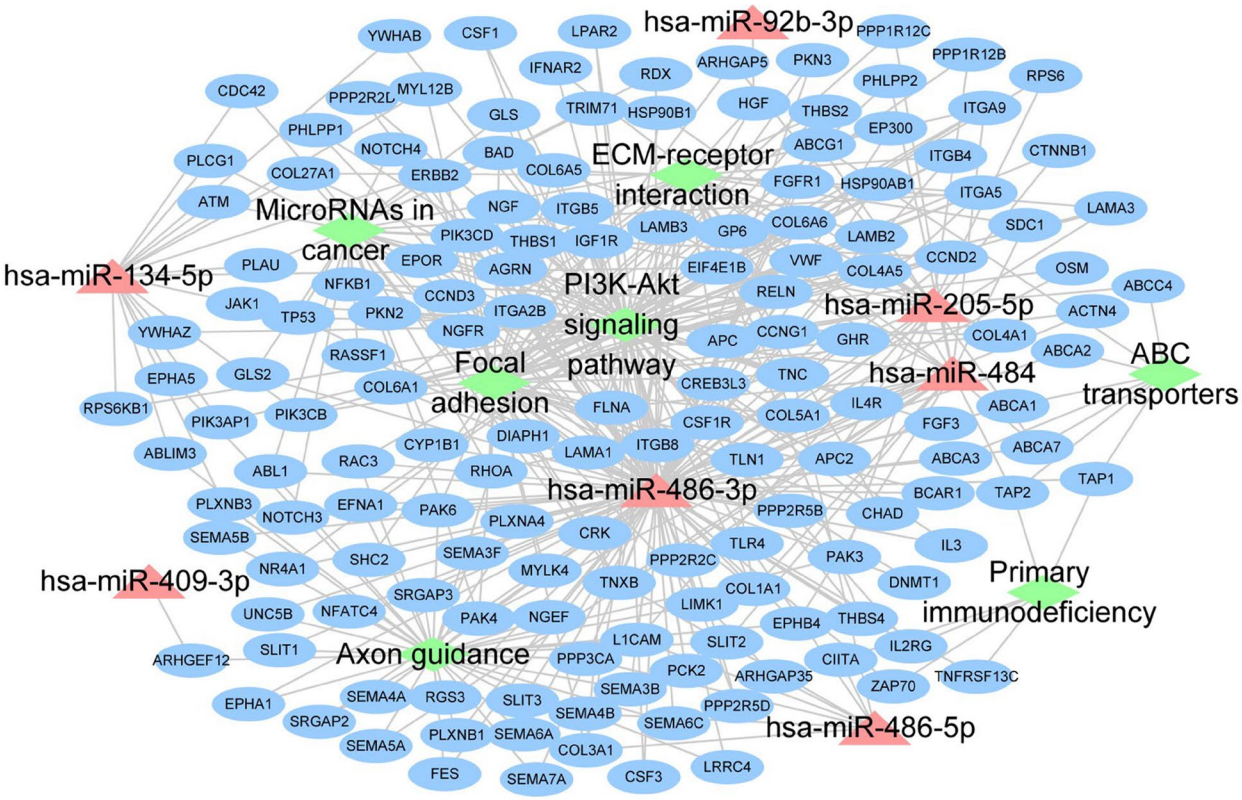


**FIGURE 4** Signaling network diagram for the prediction of genes targeted by the 7 candidate miRNAs

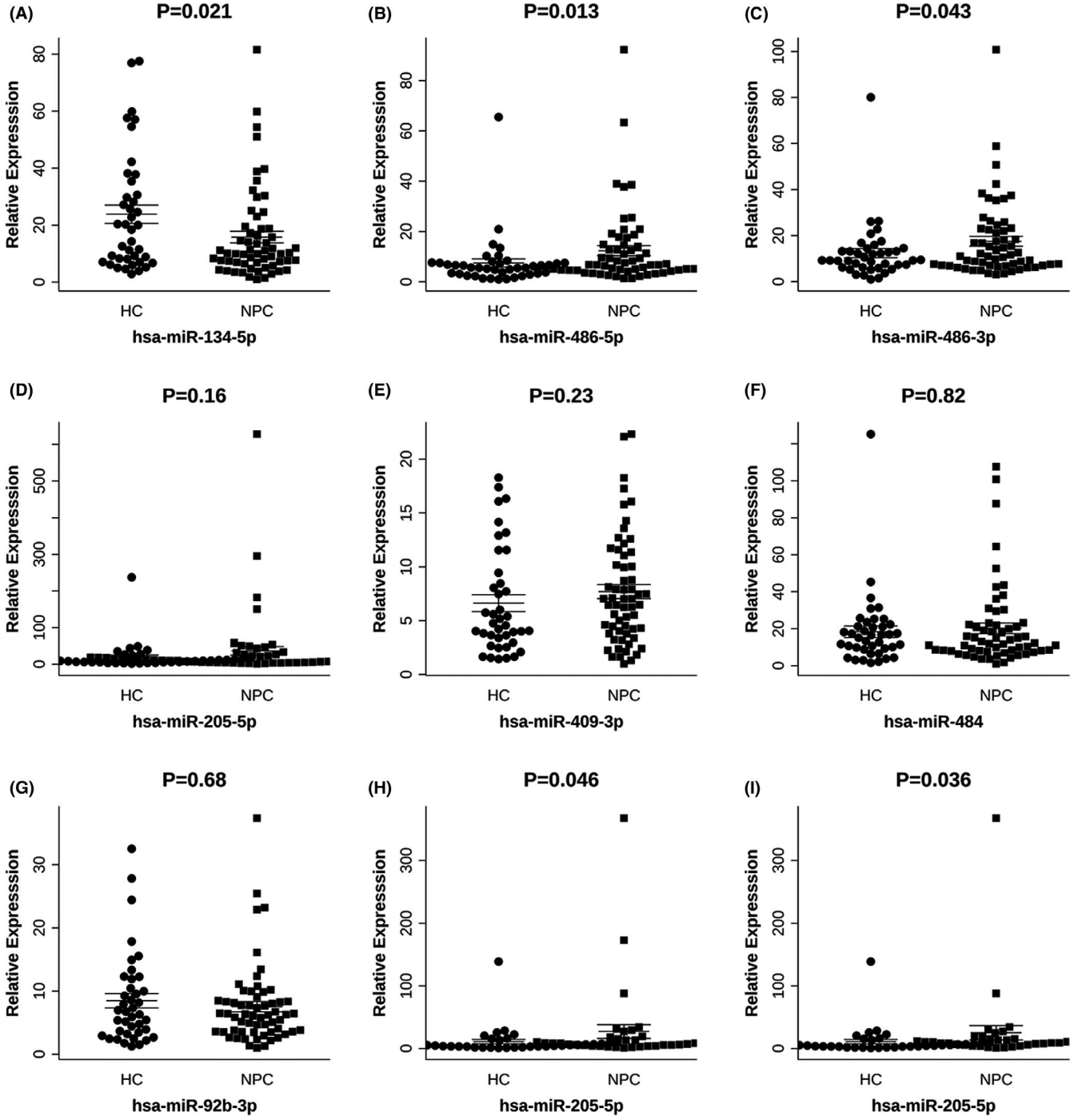


**FIGURE 5** Expression levels of selected miRNAs using qRT-PCR in the validation set. A, miR-134-5p; B, miR-486-5p; C, miR-486-3p; D, miR-205-5p; E, miR-409-3p; F, miR-484; G, miR-92b-3p. H, I, Subgroup analysis of the expression of miR-205-5p in patients with NPC and HCs. miR-205-5p expression was significantly higher in patients with advanced stage NPC (H) or EBV-positive infection (I) than that in HCs. NPC, nasopharyngeal carcinoma; HC, healthy control

### 3.3 | Selection and validation of sEV-derived miRNAs as candidate biomarkers for NPC in a validation set

To select candidate biomarkers, we constructed an UpSet plot to reveal the number of miRNAs that were common or exclusive between the groups. Considering the intersection of comparisons of 5 subgroups (NPC vs. HC, EBV-positive NPC vs. HC, EBV-negative NPC vs. HC, early-stage NPC vs HC, and advanced stage NPC vs. HC), we identified 21 miRNAs (Figure 3). We then built an assessment scale to select miRNA candidates, and comprehensively combined the differential expression and other previous NPC-associated publications to determine the score on the scale. Finally, we selected 7 miRNAs (miR-134-5p, miR-205-5p, miR-409-3p, miR-486-3p, miR-486-5p, miR-484, and miR-92b-3p) among the 21 differentially expressed miRNAs for further

**TABLE 3** Optimal performance of models containing 2 to 7 candidate miRNAs as diagnostic biomarkers for NPC

| Feature | Train SN | Train SP | Train AUC | Test SN | Test SP | Test AUC |
|---|---|---|---|---|---|---|
| miR-134-5p + miR-409-3p | 0.925 (0.825-1) | 0.64 (0.44-0.8) | 0.868 (0.773-0.963) | 0.9(0.75-1) | 0.533 (0.267-0.8) | 0.877 (0.763-0.991) |
| miR-134-5p + miR-205-5p + miR-409-3p | 0.85 (0.725-0.95) | 0.8 (0.64-0.96) | 0.882 (0.795-0.969) | 0.9(0.75-1) | 0.8 (0.6-1) | 0.91 (0.802-1) |
| miR-134-5p + miR-205-5p + miR-409-3p + miR-484 | 0.825 (0.7-0.925) | 0.84 (0.68-0.96) | 0.879 (0.791 ~ 0.967) | 0.9 (0.75 ~ 1) | 0.8 (0.6 ~ 1) | 0.91 (0.805 ~ 1) |
| miR-134-5p + miR-205-5p + miR-409-3p + miR-486-3p + miR-92b-3p | 0.8 (0.675 ~ 0.9) | 0.96 (0.88 ~ 1) | 0.895 (0.808 ~ 0.982) | 0.85 (0.7 ~ 1) | 0.867 (0.667 ~ 1) | 0.92 (0.817 ~ 1) |
| miR-134-5p + miR-205-5p + miR-409-3p + miR-484 + miR-486-3p + miR-92b-3p | 0.8 (0.675 ~ 0.925) | 0.96 (0.88 ~ 1) | 0.89(0.803 ~ 0.977) | 0.85 (0.65 ~ 1) | 0.867 (0.667 ~ 1) | 0.92 (0.817 ~ 1) |
| miR-134-5p + miR-205-5p + miR-409-3p + miR-484 + miR-486-3p + miR-486-5p + miR-92b-3p | 0.825 (0.7 ~ 0.925) | 0.92 (0.8 ~ 1) | 0.89 (0.801 ~ 0.979) | 0.85 (0.7 ~ 1) | 0.867 (0.667 ~ 1) | 0.92 (0.817 ~ 1) |

Abbreviations: SN, sensitivity; SP, specificity; AUC, area under the curve.

validation (Table 2). The enrichment pathways targeted by these 7 candidate miRNAs, based on target gene prediction, are shown in Figure 4. To validate the robustness of miRNA sequencing, we performed qPCR analysis, including an additional 60 and 40 NPC and HC samples, respectively. Compared with those in HCs, miR-134-5p was downregulated, whereas miR-486-3p and miR-486-5p were upregulated in patients with NPC (Figure 5A-G). Subgroup analysis revealed that miR-205-5p was significantly upregulated in patients with advanced stage NPC or those patients positive for EBV infection compared with that in HCs (Figure 5H-I). However, we did not observe any correlation in the validation set between the expression values of sEV-miRNAs and disease staging, EBV infection, and short-term treatment response.

### 3.4 | Construction and evaluation of sEV-derived miRNA-based model for diagnosis of nasopharyngeal carcinoma

We considered the expression values of 7 candidate sEV-derived miRNAs as a feature of subsequent analysis. We used logistic regression analysis to build a diagnostic model. The 100 participants used for constructing the model were divided randomly into 2 sets: 65 participants were used as a training set, and the remaining 35 were used as a validation set. We subsequently established the model considering both the diagnostic efficacy and the number of included candidate miRNAs. The optimal performances of models containing 2 to 7 candidate miRNAs are listed in Table 3. The model containing all 7 candidate miRNAs achieved a training AUC of 0.89 (sensitivity, 82.5%; specificity, 92.0%) and a validation AUC of 0.92 (sensitivity, 85.0%; specificity, 86.7%; Figure S2). Similarly, the model comprising 3 miRNAs (miR-134-5p, miR-205-5p, and miR-409-3p) was shown to differentiate patients with NPC from HCs with favorable diagnostic efficacy, specificity, and sensitivity (AUC of training set = 0.88, sensitivity 85%, and specificity 80%; AUC of validation set = 0.91, sensitivity 90%, and specificity 80%; Figure 6A), which was similar to the 7 miRNA-based model. Therefore, we finally selected the model comprising miR-134-5p, miR-205-5p, and miR-409-3p as a potential diagnostic biomarker. The results of the diagnostic test of the 3 miRNA-based model are shown in Table 4. We further validated the diagnostic model by comparing 4 NPC subgroups (EBV-negative, EBV-positive, early stage, and advanced stage) with HCs. As a result, we found that the model showed a good diagnostic performance, demonstrating AUC values ranging from 0.83 to 0.92 (Figure 6B). The risk probability distribution plots and the heatmap of the 3 miRNAs in the training and validation sets are shown in Figure 6C,D.

## 4 | DISCUSSION

Recently, sEVs have become a research hotspot as a noninvasive method for the diagnosis and prognosis of diseases. More specifically, sEV-derived

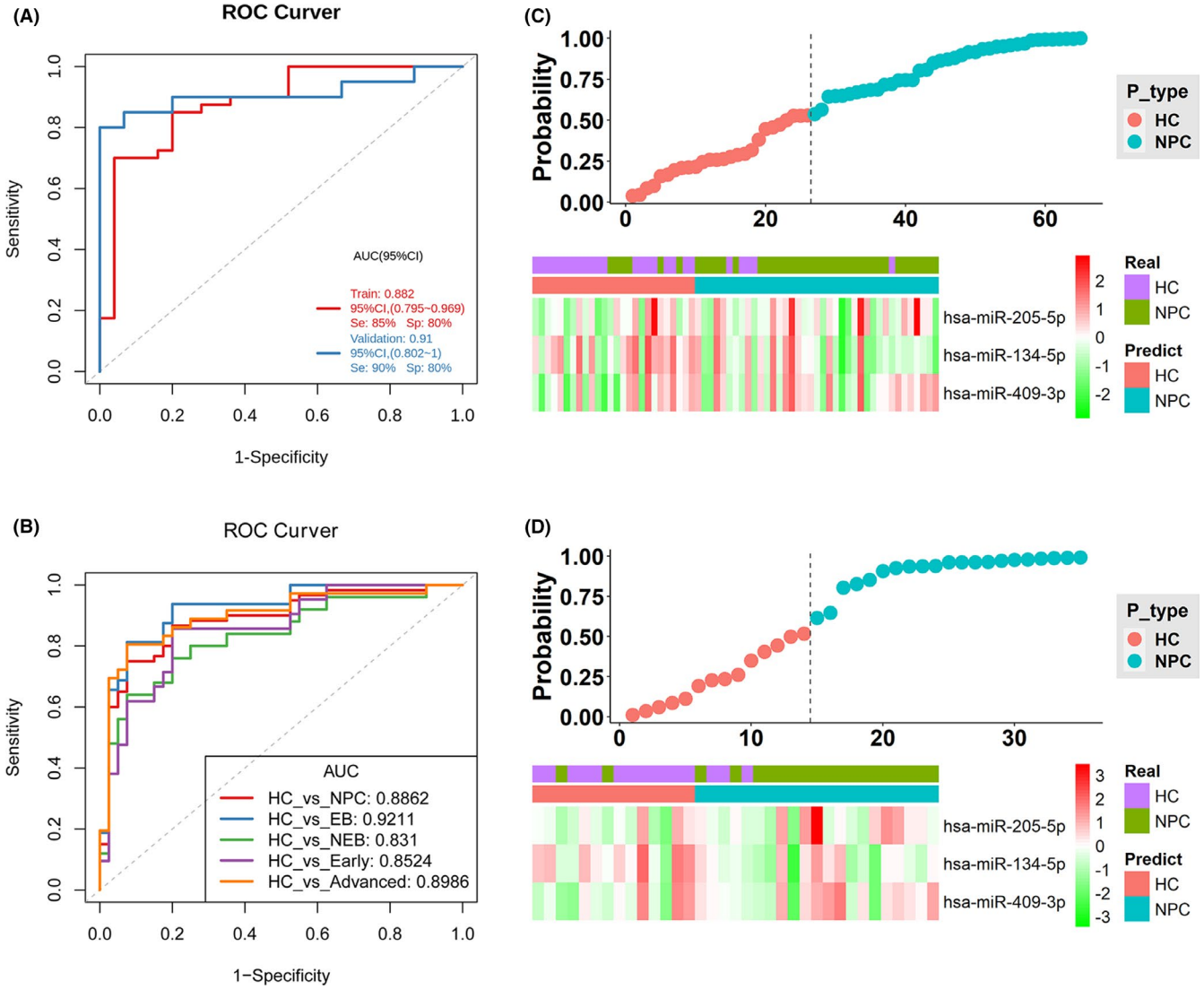


**FIGURE 6** Construction and validation of the diagnostic model based on the 3 miRNAs in the qPCR validation cohort. A, ROC curves of the 3 miRNA (miR-134-5p, miR-205-5p, miR-409-3p)-based model in the training and validation sets. B, ROC curves for the diagnosis of patients with NPC using the 3 miRNA-based model in the subgroup analysis. Risk probability distribution plots and heatmap of the 3 miRNAs in the training set (C), and validation set (D), NPC, nasopharyngeal carcinoma; HC, healthy control; EB, patients with NPC positive for Epstein-Barr virus infection; NEB, patients with NPC negative for Epstein-Barr virus infection; Early, patients with NPC diagnosed at an early stage; Advanced, patients with NPC diagnosed at an advanced stage

**TABLE 4** Diagnostic test of the 3 miRNA (miR-134-5p, miR-205-5p, and miR-409-3p)-based model for NPC

| | Training set (N = 65) | | Validation set (N = 35) | |
|---|---|---|---|---|
| | Real NPC | Real HC | Real NPC | Real HC |
| Predict NPC | 34 | 5 | 18 | 3 |
| Predict HC | 6 | 20 | 2 | 12 |
| Totals | 40 | 25 | 20 | 15 |
| Correct | 34 | 20 | 18 | 12 |
| Sensitivity (%) | 85.00% | | 90.00% | |
| Specificity (%) | | 80.00% | | 80.00% |

miRNAs have been reported to play various roles in inflammation, cell communication, tumor proliferation, angiogenesis, and metastasis, highlighting them as potential biomarkers.[16] However, few studies have explored the possibility of using sEVs for the diagnosis and prognosis of NPC. The development of NPC has been closely related to EBV infection. Some different types of circulating sEVs have been identified in NPC, including EBV-related sEVs and pure NPC-derived sEVs.[17] Moreover, previous studies have indicated that the detection of plasma cell-free EBV DNA could serve as a diagnostic biomarker of NPC.[18,19] However, due to the instability and hysteresis of the detection of EBV, finding a novel biomarker to improve the efficiency and accuracy is still necessary for patient diagnosis.[3] miRNA screening based on plasma or serum is widely used as

a noninvasive diagnostic tool and numerous studies have reported the diagnostic capacity of total RNA in the serum or plasma of patients for NPC.[20,21]

However, it should be mentioned that the free-floating circulating miRNAs and sEV-derived miRNAs in the plasma or serum are independent forms, which are distinguished from each other. A previous study identified a 5-miRNA signature for the diagnosis of NPC in serum samples, but did not observe any significant differences for any of the 5 miRNAs in serum-derived exosome samples.[12] A study by Min et al compared the RNA in plasma sEV-derived miRNAs to the total miRNA in plasma.[22] Their results revealed that the abundance and composition of sEV-derived miRNAs were dramatically different from those of plasma total miRNAs. This phenomenon might be explained by the discrepancy between the expression of miRNAs in the serum or plasma and extracellular vesicles. Cellular miRNAs are selectively sorted into vesicles through specific processes.[23,24] In contrast, the majority of circulating miRNAs is known to be loaded in proteins as ribonucleoprotein complexes rather than extracellular vesicles, which are sensitive to proteinase digestion in the plasma or serum.[25]

In brief, plasma sEV-derived miRNAs have not yet been used as effective biomarkers of NPC in the clinical setting. It is therefore critical to identify sEV-miRNAs as biomarkers that might be helpful in the diagnosis of NPC.

Here, we performed a comprehensive study of sEV-derived miRNAs to explore their significance as novel biomarkers of NPC. We isolated sEVs from plasma using a SEC method and identified DEMs in sEVs using next-generation sequencing. Based on the comparison of the intersection of 5 subgroups (NPC vs. HC, EBV-positive NPC vs. HC, EBV-negative NPC vs. HC, early-stage NPC vs HC, and advanced stage NPC vs. HC), we selected a total of 21 overlapping miRNAs. In the miRNA screening phase, we considered 7 of these 21 miRNAs as underlying diagnostic biomarkers for NPC, of which 3 miRNAs (miR-134-5p, miR-409-3p, and miR-92b-3p) were found to be downregulated, whereas 4 miRNAs (miR-205-5p, miR-484, miR-486-3p, and miR-486-5p) were shown to be upregulated. Compared with that in HCs, the expression of miR-134-5p in patients with NPC in the validation cohort was significantly decreased, whereas that of miR-486-3p and miR-486-5p was significantly increased. In addition, we detected that miR-205 was significantly upregulated in the subgroup of patients with advanced stage NPC and EBV infection compared with that in HCs. Nevertheless, we did not observe any significant differences in the expression level of miR-409-3p, miR-484, and miR-92b between patients with NPC and HCs that might be attributed to the small sample size used in this study. We then included the 7 selected sEV-derived miRNAs in the construction of a diagnostic model using logistic regression. Finally, we selected a 3 miRNA (miR-134-5p, miR-205-5p, and miR-409-3p)-based model based on its diagnostic performance and feasibility. Furthermore, our ROC analysis of the 3 miRNA-based model indicated a favorable AUC value, suggesting that it might help in the diagnosis of NPC.

The expression of sEV-derived NPC miRNAs in our study was consistent with that reported in previous studies. miR-134-5p potentially acts as a tumor suppressor, repressing the proliferation of NPC cells by directly targeting E74-like ETS transcription factor 2 (ELF2).[26] Decreasing the expression of miR-134-5p was also suggested to promote radioresistance by the P21 and AKT/GSK-3β/β-catenin pathway.[27] In our study, the predicted genes targeted by miR-134-5p included *ATM* and *JAK1*, both of which have been associated with NPC. Several studies have revealed that ATM mediates DNA repair and activates the resistance of NPC cells to radiotherapy or chemotherapy by the ATM-associated signaling pathway.[28-31] The JAK1/STAT3 pathway plays a critical role in the progression of NPC.[32] Similarly, miR-205-5p has been demonstrated to be upregulated in NPC tissues or plasma and may be considered a potential diagnostic biomarker.[33,34] Furthermore, miR-205-5p is critical to the progression and chemotherapy resistance of NPC due to its regulation of EMT by targeting phosphatase and tensin homolog (PTEN) through the PI3K/AKT signaling pathway.[35] Moreover, cyclin D2, a cell cycle-related gene, targeted by miR-205-5p in our study, has been suggested to affect the proliferation of NPC cells, G1/S transition, and metastasis.[36,37] However, there is still a lack of research on the relationship between miR-409-3p and NPC. Previous studies have indicated that miR-409-3p regulates the proliferation, migration, invasion, and apoptosis of various cancers.[38,39] miR-409-3p may also be considered a biomarker in lung adenocarcinoma and prostate cancer.[40,41] Some studies have reported that miR-486-3p promotes cell invasion and tumor progression through the activation of cancer-associated signaling pathways in NPC and other various types of cancer.[42,43] Additionally, miR-486-3p is a member of the regulatory network associated with the pathophysiology of NPC.[44] Although the role of miR-486-5p in NPC has not been reported previously, it may serve as a biomarker for the recurrence of oral squamous cell carcinoma after operation.[45] Previous studies have revealed that miR-486-5p mediates the cell proliferation, apoptosis, and chemosensitivity of certain cancers.[46,47] Furthermore, Hu et al have indicated that small vesicular-derived miR-486-5p regulates the cell cycle, proliferation, and metastasis in lung adenocarcinoma through NIMA-related kinase 2 (NEK2).[48]

The interactions between NPC cells and the tumor microenvironment are critical and have been shown to rely on sEV-derived miRNAs. An increase in the release of sEVs and an imbalance in sEV-derived miRNAs could modulate the gene expression involved in the development of NPC.[49] Reportedly, the sEV-derived miRNAs released from resistant NPC cells might transfer into sensitive NPC cells.[50] Furthermore, sEVs from cancer-associated fibroblasts surrounding the cancer cells could also induce a resistant phenotype by affecting the cell growth, EMT, and apoptosis.[51-53] Additionally, sEVs have been demonstrated to promote the resistance of NPC to radiotherapy by P38 MAPK signaling.[54] Therefore, as sEV-miRNAs play a crucial role in cancer development and progression, miRNA expression signatures may be used as potential diagnostic biomarkers.

In summary, our findings revealed that circulating sEV-derived miRNA profiles in patients with NPC were different from those in HCs. Among the candidate miRNAs, miR-134-5p, miR-205-5p, miR-486-5p,

and miR-486-3p were significantly dysregulated in NPC compared with those in HC in the validation cohort. Furthermore, a diagnostic model comprising miR-134-5p, miR-205-5p, and miR-409-3p was established using logistic regression analysis. Finally, the 3 miRNA-based model showed good diagnostic capabilities for the detection and prognosis of NPC. However, our findings are preliminary and need further verification in future large-scale and multicenter trials.

## ACKNOWLEDGMENTS

This study was supported by Middle-aged and Young Teachers' Basic Ability Promotion Project of Guangxi (No. 2018KY0134), Guangxi Medical and Health Appropriate Technology Development and Promotion Application Project (No. S2017020), the Key Research and Development Program of Guangxi (No. Guike AB18281003), the "139" Program for high-level medical talents in Guangxi, Innovation Team of the First Affiliated Hospital of Guangxi Medical University, Guangxi Science and Technology Program Project (GK AD17129013), and the National Natural Science Foundation of China (Nos. 82060019, 82060494). The funders had no role in the study design, data collection and analysis, decision to publish, or preparation of the manuscript. We thank Zhigang Zheng and Guanyi Kong (Echo Biotech Co., Ltd at Beijing, China) for helpful discussions and bioinformatics analysis.

## DISCLOSURE

The authors declare no competing interests (both financial and non-financial).

## DATA AVAILABILITY STATEMENT

The datasets presented in this study can be found in online repositories. The miRNA sequencing data can be found in SRA (https://www.ncbi.nlm.nih.gov/sra/) and the SRA ID is PRJNA706896.

## ORCID

*Fang Wu* https://orcid.org/0000-0003-3806-1872

## REFERENCES

1. Chen W, Zheng R, Baade PD, et al. Cancer statistics in China, 2015. *CA Cancer J Clin*. 2016;66:115-132.
2. Mao YP, Xie FY, Liu LZ, et al. Re-evaluation of 6th edition of AJCC staging system for nasopharyngeal carcinoma and proposed improvement based on magnetic resonance imaging. *Int J Radiat Oncol Biol Phys*. 2009;73:1326-1334.
3. Zhang J, Shi H, Jiang T, Liu Z, Lin PP, Chen N. Circulating tumor cells with karyotyping as a novel biomarker for diagnosis and treatment of nasopharyngeal carcinoma. *BMC Cancer*. 2018;18:1133.
4. An T, Qin S, Xu Y, et al. Exosomes serve as tumour markers for personalized diagnostics owing to their important role in cancer metastasis. *J Extracell Vesicles*. 2015;4:27522.
5. Kamerkar S, LeBleu VS, Sugimoto H, et al. Exosomes facilitate therapeutic targeting of oncogenic KRAS in pancreatic cancer. *Nature*. 2017;546:498-503.
6. Zhang H, Deng T, Liu R, et al. Exosome-delivered EGFR regulates liver microenvironment to promote gastric cancer liver metastasis. *Nat Commun*. 2017;8:15016.
7. Valadi H, Ekström K, Bossios A, Sjöstrand M, Lee JJ, Lötvall JO. Exosome-mediated transfer of mRNAs and microRNAs is a novel mechanism of genetic exchange between cells. *Nat Cell Biol*. 2007;9:654-659.
8. Vlaeminck-Guillem V. Extracellular vesicles in prostate cancer carcinogenesis, diagnosis, and management. *Front Oncol*. 2018;8:222.
9. Rodrigues-Junior DM, Tan SS, de Souza VL, et al. A preliminary investigation of circulating extracellular vesicles and biomarker discovery associated with treatment response in head and neck squamous cell carcinoma. *BMC Cancer*. 2019;19:373.
10. Drula R, Ott LF, Berindan-Neagoe I, Pantel K, Calin GA. MicroRNAs from liquid biopsy derived extracellular vesicles: recent advances in detection and characterization methods. *Cancers (Basel)*. 2020;12:2009.
11. Aga M, Bentz GL, Raffa S, et al. Exosomal HIF1α supports invasive potential of nasopharyngeal carcinoma-associated LMP1-positive exosomes. *Oncogene*. 2014;33:4613-4622.
12. Zou X, Zhu D, Zhang H, et al. MicroRNA expression profiling analysis in serum for nasopharyngeal carcinoma diagnosis. *Gene*. 2020;727:144243.
13. Théry C, Amigorena S, Raposo G, Clayton A. Isolation and characterization of exosomes from cell culture supernatants and biological fluids. *Curr Protoc Cell Biol*. 2006;30(1):3.22.1–3.22.29. https://doi.org/10.1002/0471143030.cb0322s30
14. Mao X, Cai T, Olyarchuk JG, Wei L. Automated genome annotation and pathway identification using the KEGG Orthology (KO) as a controlled vocabulary. *Bioinformatics*. 2005;21:3787-3793.
15. Xie C, Mao X, Huang J, et al. KOBAS 2.0: a web server for annotation and identification of enriched pathways and diseases. *Nucleic Acids Res*. 2011;39:W316-322.
16. Mao L, Li X, Gong S, et al. Serum exosomes contain ECRG4 mRNA that suppresses tumor growth via inhibition of genes involved in inflammation, cell proliferation, and angiogenesis. *Cancer Gene Ther*. 2018;25:248-259.
17. Harmati M, Tarnai Z, Decsi G, et al. Stressors alter intercellular communication and exosome profile of nasopharyngeal carcinoma cells. *J Oral Pathol Med*. 2017;46:259-266.
18. Liu W, Li H, Sheng H, et al. A Randomized Controlled Trial on Evaluation of Plasma Epstein-Barr Virus Biomarker for Early Diagnosis in Patients With Nasopharyngeal Carcinoma. *Adv Ther*. 2020;37(10):4280–4290.
19. Anh VNQ, Van Ba N, Anh DT, et al. Validation of a highly sensitive qPCR assay for the detection of plasma cell-free epstein-barr virus dna in nasopharyngeal carcinoma diagnosis. *Cancer Control*. 2020;27:1073274820944286.
20. Are E, Irekeola AA, Yean YC. Diagnostic and prognostic indications of nasopharyngeal carcinoma. *Diagnostics (Basel)*. 2020;10(9):611.
21. Liu L, Wang H, Yan C, Tao S. An integrated analysis of mRNAs and miRNAs microarray profiles to screen miRNA signatures involved in nasopharyngeal carcinoma. *Technol Cancer Res Treat*. 2020;19:1533033820956998.
22. Min L, Zhu S, Chen L, et al. Evaluation of circulating small extracellular vesicles derived miRNAs as biomarkers of early colon cancer: a comparison with plasma total miRNAs. *J Extracell Vesicles*. 2019;8:1643670.
23. Janas T, Janas MM, Sapoń K, Janas T. Mechanisms of RNA loading into exosomes. *FEBS Lett*. 2015;589:1391-1398.
24. Villarroya-Beltri C, Baixauli F, Gutiérrez-Vázquez C, Sánchez-Madrid F, Mittelbrunn M. Sorting it out: regulation of exosome loading. *Semin Cancer Biol*. 2014;28:3-13.
25. Arroyo JD, Chevillet JR, Kroh EM, et al. Argonaute2 complexes carry a population of circulating microRNAs independent of vesicles in human plasma. *Proc Natl Acad Sci U S A*. 2011;108:5003-5008.
26. Liu Y, Tao Z, Qu J, Zhou X, Zhang C. Long non-coding RNA PCAT7 regulates ELF2 signaling through inhibition of miR-134-5p in nasopharyngeal carcinoma. *Biochem Biophys Res Commun*. 2017;491:374-381.

27. Zuo Z, Ji S, He L, Zhang Y, Peng Z, Han J. LncRNA TTN-AS1/miR-134-5p/PAK3 axis regulates the radiosensitivity of human large intestine cancer cells through the P21 pathway and AKT/GSK-3β/β-catenin pathway. *Cell Biol Int*. 2020;44(11):2284–2292.
28. Sun L, Wu C, Ming J, et al. Riluzole enhances the response of human nasopharyngeal carcinoma cells to ionizing radiation via ATM/P53 signalling pathway. *J Cancer*. 2020;11:3089-3098.
29. Zhou X, Zheng J, Tang Y, et al. EBV encoded miRNA BART8-3p promotes radioresistance in nasopharyngeal carcinoma by regulating ATM/ATR signaling pathway. *Biosci Rep*. 2019;39(9):BSR20190415. https://doi.org/10.1042/BSR20190415
30. Nie X, Guo E, Wu C, et al. SALL4 induces radioresistance in nasopharyngeal carcinoma via the ATM/Chk2/p53 pathway. *Cancer Med*. 2019;8:1779-1792.
31. Li D, Ye L, Lei Y, Wan J, Chen H. Downregulation of FoxM1 sensitizes nasopharyngeal carcinoma cells to cisplatin via inhibition of MRN-ATM-mediated DNA repair. *BMB Rep*. 2019;52:208-213.
32. Zhang X, Yang J, Bian Z, Shi D, Cao Z. Long noncoding RNA DANCR promotes nasopharyngeal carcinoma progression by interacting with STAT3, enhancing IL-6/JAK1/STAT3 signaling. *Biomed Pharmacother*. 2019;113:108713.
33. Zhang H, Zou X, Wu L, et al. Identification of a 7-microRNA signature in plasma as promising biomarker for nasopharyngeal carcinoma detection. *Cancer Med*. 2020;9:1230-1241.
34. Luan J, Wang J, Su Q, Chen X, Jiang G, Xu X. Meta-analysis of the differentially expressed microRNA profiles in nasopharyngeal carcinoma. *Oncotarget*. 2016;7:10513-10521.
35. Zhang P, Lu X, Shi Z, et al. miR-205-5p regulates epithelial-mesenchymal transition by targeting PTEN via PI3K/AKT signaling pathway in cisplatin-resistant nasopharyngeal carcinoma cells. *Gene*. 2019;710:103-113.
36. Li X, Liu F, Lin B, et al. miR-150 inhibits proliferation and tumorigenicity via retarding G1/S phase transition in nasopharyngeal carcinoma. *Int J Oncol*. 2017;50:1097-1108.
37. Xu S, Zhao N, Hui L, Song M, Miao ZW, Jiang XJ. MicroRNA-124-3p inhibits the growth and metastasis of nasopharyngeal carcinoma cells by targeting STAT3. *Oncol Rep*. 2016;35:1385-1394.
38. Long Z, Gong F, Li Y, Fan Z, Li J. Circ_0000285 regulates proliferation, migration, invasion and apoptosis of osteosarcoma by miR-409-3p/IGFBP3 axis. *Cancer Cell Int*. 2020;20:481.
39. Yin D, Hua L, Wang J, Liu Y, Li X. Long non-coding RNA DUXAP8 facilitates cell viability, migration, and glycolysis in non-small-cell lung cancer via regulating HK2 and LDHA by inhibition of miR-409-3p. *Onco Targets Ther*. 2020;13:7111-7123.
40. Wang J, Zhang C, Peng X, et al. A combination of four serum miRNAs for screening of lung adenocarcinoma. *Hum Cell*. 2020;33:830-838.
41. Fredsøe J, Rasmussen AKI , Mouritzen P, et al. Profiling of circulating microRNAs in prostate cancer reveals diagnostic biomarker potential. *Diagnostics (Basel)*. 2020;10(4):188. https://doi.org/10.3390/diagnostics10040188
42. Liang H, Huang H, Li Y, Lu Y, Ye T. CircRNA_0058063 functions as a ceRNA in bladder cancer progression via targeting miR-486-3p/FOXP4 axis. *Biosci Rep*. 2020;40(3):BSR20193484. https://doi.org/10.1042/BSR20193484
43. Chen L, Xiong L, Hong S, et al. Circulating myeloid-derived suppressor cells facilitate invasion of thyroid cancer cells by repressing miR-486-3p. *J Clin Endocrinol Metab*. 2020;105(8):2704–2718.
44. Zhou DN, Ye CS, Yang QQ, Deng YF. Integrated analysis of transcriptome profiling predicts potential lncRNA and circRNA targets in human nasopharyngeal carcinoma. *Oncol Lett*. 2020;19:3123-3136.
45. Yan Y, Wang X, Venø MT, et al. Circulating miRNAs as biomarkers for oral squamous cell carcinoma recurrence in operated patients. *Oncotarget*. 2017;8:8206-8214.
46. Zhang Y, Han G, Cao Y, Zhang Y, Zhang X, Gong H. Solasonine inhibits gastric cancer proliferation and enhances chemosensitivity through microRNA-486-5p. *Am J Transl Res*. 2020;12:3522-3530.
47. Salimian J, Baradaran B, Azimzadeh Jamalkandi S, Moridikia A, Ahmadi A. MiR-486-5p enhances cisplatin sensitivity of human muscle-invasive bladder cancer cells by induction of apoptosis and down-regulation of metastatic genes. *Urol Oncol*. 2020;38(738):e739-738.e721.
48. Hu H, Xu H, Lu F, et al. Exosome-Derived miR-486-5p regulates cell cycle, proliferation and metastasis in lung adenocarcinoma via targeting NEK2. *Front Bioeng Biotechnol*. 2020;8:259.
49. Zhou Y, Xia L, Lin J, et al. Exosomes in Nasopharyngeal Carcinoma. *J Cancer*. 2018;9:767-777.
50. Kalluri R. The biology and function of exosomes in cancer. *J Clin Invest*. 2016;126:1208-1215.
51. Hu Y, Yan C, Mu L, et al. Fibroblast-derived exosomes contribute to chemoresistance through priming cancer stem cells in colorectal cancer. *PLoS One*. 2015;10:e0125625.
52. Chen WX, Liu XM, Lv MM, et al. Exosomes from drug-resistant breast cancer cells transmit chemoresistance by a horizontal transfer of microRNAs. *PLoS One*. 2014;9:e95240.
53. Malla B, Zaugg K, Vassella E, Aebersold DM, Dal Pra A. Exosomes and exosomal micrornas in prostate cancer radiation therapy. *Int J Radiat Oncol Biol Phys*. 2017;98:982-995.
54. Zhang Z, Yu X, Zhou Z, et al. LMP1-positive extracellular vesicles promote radioresistance in nasopharyngeal carcinoma cells through P38 MAPK signaling. *Cancer Med*. 2019;8:6082-6094.


## SUPPORTING INFORMATION

Additional supporting information may be found online in the Supporting Information section.

**How to cite this article:** Jiang L, Zhang Y, Li B, et al. miRNAs derived from circulating small extracellular vesicles as diagnostic biomarkers for nasopharyngeal carcinoma. *Cancer Sci*. 2021;112:2393–2404. https://doi.org/10.1111/cas.14883